J Sol-Gel Sci Technol (2007) 44:29–40
DOI 10.1007/s10971-007-1598-7

ORIGINAL PAPER

Polydicyclopentadiene based aerogel: a new insulation material

Je Kyun Lee · George L. Gould

Received: 5 March 2007 / Accepted: 26 June 2007 / Published online: 19 July 2007

Abstract Lightweight polydicyclopentadiene (pDCPD) based aerogels were developed via a simple sol-gel processing and supercritical drying method. The uniform pDCPD wet gels were first prepared at room temperature and atmospheric pressure through ring opening metathesis polymerization (ROMP) incorporating homogeneous ruthenium catalyst complexes (Grubbs catalyst). Gelation kinetics were significantly affected by both catalyst content and target density (i.e., solid content), while gel solvents also played important role in determining the appearance and uniformity of wet gel and aerogel products. A supercritical carbon dioxide (CO_2) drying method was used to extract solvent from wet pDCPD gels to afford nanoporous aerogel solid. A variety of pDCPD based aerogels were synthesized by varying target density, catalyst content, and solvent and were compared with their xerogel analogs (obtained by ambient pressure solvent removal) for linear shrinkage and thermal conductivity value (1 atm air, 38 °C mean temperature). Target density played a key role in determining porosity and thermal conductivity of the resultant pDCPD aerogel. Differential scanning calorimetery (DSC) demonstrated that the materials as produced were not fully-crosslinked. The pDCPD based aerogel monoliths demonstrated high porosities, low thermal conductivity values, and inherent hydrophobicity. These aerogel materials are very promising candidates for many thermal and acoustic insulation applications including cryogenic insulation.

J. K. Lee (✉) · G. L. Gould
Research and Development Division, Aspen Aerogels, Inc.,
30 Forbes Road, Building B, Northborough, MA 01532, USA
e-mail: jekyun@aerogel.com

G. L. Gould
e-mail: ggould@aerogel.com

Keywords Polydicyclopentadiene (pDCPD) · Aerogels · Ring opening metathesis polymerization (ROMP) · Supercritical drying · Nanoporous · Insulation

1 Introduction

Aerogels invented in 1931 by Kistler [1, 2] were formed from a gel by replacing the liquid phase with air. The first aerogels produced by Kistler had silicon dioxide (silica) as the solid phase of the gel structure. Silica gels can be formed via polymerization of silicic acid ($Si(OH)_4$). Silica aerogels prepared via sol-gel processing can exhibit extremely low density, high surface area, and attractive optical, dielectric, thermal and acoustic properties [3, 4]. These excellent properties explain why aerogels have been considered for use in thermal and acoustic insulation applications [5–12].

Aerogel materials are typically prepared by removing the solvent contained in a gel matrix by extraction in a supercritical fluid medium. This can be accomplished by bringing the gel solvent system above its critical temperature and pressure and subsequently relieving pressure above the critical temperature until only vapor remains. Alternatively, the gel solvent system can be extracted by contacting the wet gel with an appropriate solvent. One popular extraction solvent is carbon dioxide because it is inexpensive and has a relatively low critical temperature (31 °C) and critical pressure of 73 atm (7.3 MPa) [8, 9, 11, 12]. During supercritical drying, the temperature and the pressure are increased beyond the solvent critical point, and therefore where the phase boundary between the liquid and vapor phase disappears. Once the critical point is passed, there is no distinction between the liquid and vapor phase and the solvent can be removed without introducing a

liquid–vapor interface, capillary pressure or any associated mass transfer limitations. This step is controlled by two important phenomena: permeability and capillary stress [8, 9, 11, 12]. The general preparation methods, the unique physical and thermal properties, and future potential applications of aerogels can be found in some of outstanding review papers [8–12]. Aerogel-like materials can also be produced by drying a wet gel at ambient pressure. The ambient pressure drying process is called the "xerogel" process, and produces a material with aerogel like properties from an organic or inorganic based wet gel by driving solvent out of a gelled matrix. The ambient pressure drying process generally induces more shrinkage and damage of pore structure due to high capillary forces, and typically requires relatively long drying periods as the volume of the porous gel increases.

Nanoporous aerogel materials have also been derived from organic polymers, some of which can be converted to carbon based aerogels. A good introduction to organic polymer based aerogels (organic aerogels) can be found in a paper by Pekala and Schaefer [13]. Kistler was the first to prepare the organic aerogels with natural products and their derivatives [1, 2]. Pekala and co-workers have intensively studied organic aerogels mainly related to Resorcinol/Formaldehyde (RF), Melamine/Formaldehyde (MF), and Phenolic/Furfural (PF) [13–20]. These RF, MF, and PF organic aerogels can be converted into carbon aerogels through pyrolysis. Polyurethane based organic xerogels, aerogels, and subsequently derived carbon aerogels were prepared using by drying at ambient or supercritical condition followed by inert atmosphere pyrolysis [21–23]. On the other hand, Tan et al. [24] recently reported cellulose based aerogels with significantly improved impact strength, while Fischer et al. [25] investigated an alternate cellulose aerogel that incorporated a non-toxic polyisocyanate crosslinking agent. Tan et al. [24] reported very high impact strength from their cellulose aerogel samples prepared by using toluene diisocyanate (TDI) crosslinker, while Fischer et al. [25] didn't find any significant difference of the compression mechanical properties between their cellulose acetate aerogel and RF aerogels.

Although silica aerogels demonstrate many unusual and useful properties, their commercialization has so far been rather limited because of their relatively low strength, brittleness, and high cost. Organic aerogel commercialization for industrial applications has also been slow, most likely due to utilization of toxic constituent components (isocyanates, formaldehyde)[1] in their manufacture, relatively high precursor prices, and/or complex processing requirements (inert atmosphere pyrolysis to make carbonized aerogels).

[1] http://www.osha.gov/SLTC/formaldehyde/recognition.html

Dicyclopentadiene (DCPD) is a readily available byproduct in the petrochemical industry and thus is relatively inexpensive. The DCPD monomer contains a strained ring that can be polymerized via a ring-opening metathesis polymerization (ROMP) reaction and converted into a crosslinked polymer material with excellent mechanical properties (high compressive modulus and high tensile strength) and little chemical shrinkage [26, 27]. The recently developed Grubbs' type ruthenium-based ROMP catalyst systems have been widely demonstrated to show high metathesis activity and tolerance of a wide range of functional groups as well as oxygen and water [28, 29]. This unique homogeneous catalyst system is able to polymerize DCPD monomer into robust polymer materials with a number of unique and desirable properties suitable for many aerospace and transportation applications. Using Grubbs' type ruthenium catalyst, we recently carried out an experimental investigation [30] on developing a new type of organic aerogel product. The gel formation, thermal conductivity value, porosity and pore morphology and structure, and thermal properties of the first pDCPD based aerogels were discussed as functions of material variables such as target density and catalyst contents. The primary objective of this study is to understand the feasibility to develop low cost, lightweight nanostructured pDCPD based aerogel and their preparation method.

2 Experimental

Commercially available DCPD monomer, Grubbs catalyst, and solvents were used for aerogel sample preparation. High purity DCPD monomer (D2384; 98% pure) was purchased from Spectrum. The DCPD resin is a mixture of solid and liquid at room temperature due to its low melting point and is easily dissolved in different solvents including toluene, MEK, acetone, 2-propanol and ethanol forming a clear solution. However, although most solvents dissolved the DCPD resin directly, very small particulates or globules of resin were observed upon attempted dissolution in polar solvents such as ethanol and 2-propanol. Clearer solutions and more uniform wet gels were obtained when less polar solvents such as toluene and hexane were used. Bis(tricyclohexylphosphine)-3-phenyl-1H-inden-1-ylideneruthenium dichloride was purchased from STREM Chemical and used as a ROMP catalyst. These Grubbs catalysts are soluble in most common organic solvents giving clear light or dark brown color solutions depending on the solvent type. All solvents were purchased as reagent grade from Aldrich and used as received without further purification. Toluene was mostly used for the gelation solvent due to the uniform wet gel formation and acetone was used for the aging solvent, unless otherwise noted. The sample preparation

procedure for pDCPD based aerogel monoliths is illustrated in Fig. 1. All formulations were produced at roughly ambient conditions, gelled, and aged at room temperature for 1–2 weeks, unless otherwise noted. The Grubbs catalyst didn't appear to show any air or moisture sensitivity, as reported in previous studies [26–29]. The pDCPD based aerogels were produced from their wet gels by drying in supercritical CO_2. For comparison purposes, xerogels were prepared by slow evaporation of solvents in a hood at ambient conditions.

Basic properties of the gel systems, including gel time, bulk density, shrinkage factor, thermal conductivity at atmospheric conditions, thermal transition behaviors, pore morphology, and pore volume and size distribution were measured. Gel time was defined as the time period following addition of all catalyst into the sol, to the gelation point of the sol where sample did not move with gentle shaking. The shrinkage factor is defined as the ratio of the final density of the dried samples to the target density calculated from solid content in the sol: Shrinkage Factor (f) = Final Density (g/cm^3)/Target Density (g/cm^3). Also, as used in [31], the overall porosity (%) was calculated using pDCPD material density of 1.064 g/cc: Porosity (%) = 100 – [[bulk pDCPD aerogel density (g/cm^3)/material (pDCPD) density (g/cm^3)] × 100]. Thermal conductivity at a single mean temperature was measured using a custom heat flow meter at room temperature and ambient pressure, as schematically demonstrated in Fig. 2. Test equipment consists of a hot plate, a NIST-calibrated reference sample (i.e., polystyrene), aerogel sample for measurement, and thermocouples. The thermal conductivity coefficients were obtained by a one-dimensional Fourier–Biot law: $q = -\lambda\,(dT/dx)$, where q is heat flux (W/m^2), λ is thermal conductivity coefficient (W/m K), and dT/dx is temperature gradient (K/m) on the isotherm flat surface. Nanopore structure information such as nanopore size, BET surface area, nanopore volume, and pore size distribution were measured by using liquid nitrogen absorption method in Accelerated Surface Area and Porosimetry Measurement System (Micromeritics Instrument Co., Model: ASAP 2010) after degassing at 70 °C (105 °C for silica aerogel) for 12 h. Pore morphologies were measured by using a field-emission scanning electron microscope (FESEM, JEOL JSM-6335F). The fracture surface of each sample was used for FESEM measurements. Before measurement, the samples were made conductive by coating the surface with 25 nm of Platinum/Palladium (Pt/Pd) alloy. FESEM observations were conducted at an accelerating voltage of 5 kV and 8 mm working distance and a #4 aperture. The morphology pictures were taken at the different magnifications and the measurement uncertainty of the scale bar of FESEM is known to be 14% at 95% confidence. Thermal transition behaviors such as glass transition temperature (T_g), curing reaction peak and temperature, and thermal degradation temperatures were measured using thermal analysis equipment of Mettler Toledo FP90 Central Processor with FP 99A analysis software.

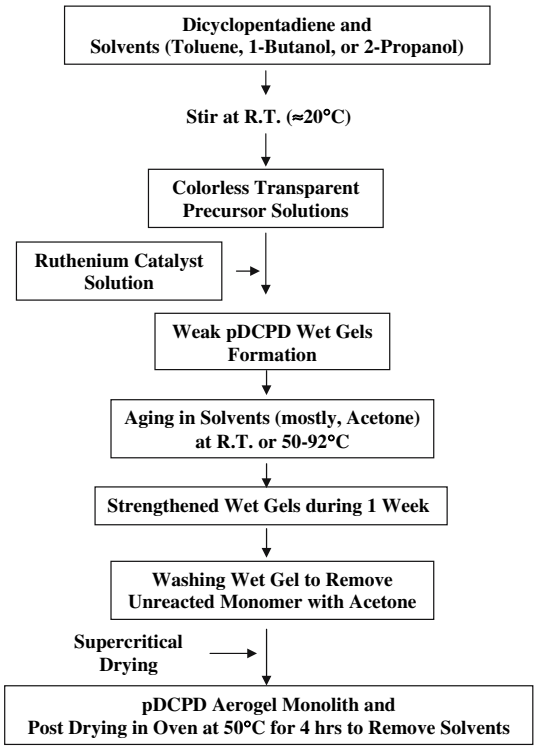

Fig. 1 Flow chart for the preparation procedure of pDCPD aerogel monoliths

The effect of the Grubbs catalyst content on the important properties of the resultant samples was first studied at a constant target density of 0.06 g/cm^3. The detailed recipes used for the experiments are summarized in Table 1. Next, the relationship between the target density and the gelation kinetics was investigated at a constant Grubbs catalyst content as a ratio of Catalyst/DCPD (wt/wt) = 0.003. It is well known to aerogel researchers that the target density (i.e., solid content) is one of the most

Fig. 2 Demonstration of the linear and crosslinked polymers resulted from ROMP reaction of DCPD monomers

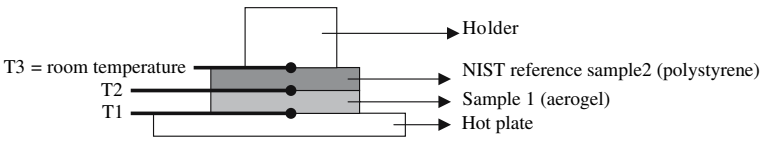

Table 1 Recipes used to study the effect of the Grubbs catalyst content on the important properties of the resultant pDCPD aerogels prepared with a constant target density of 0.06 g/cm^3

Experiment number	ρ_{Target} (g/cm^3)	Grubbs catalyst/DCPD (wt/wt)
Exp-C1	0.06	0.0025
Exp-C2	0.06	0.005
Exp-C3	0.06	0.01
Exp-C4	0.06	0.025
Exp-C5	0.06	0.05

Table 2 Recipes used to study the effect of the target density on the important properties of the resultant pDCPD aerogels prepared with a constant Grubbs catalyst content of catalyst/DCPD (wt/wt) = 0.003

Experiment number	ρ_{Target} (g/cm^3)	Catalyst/DCPD (wt/wt)
Exp-T1	0.02	0.003
Exp-T2	0.04	0.003
Exp-T3	0.07	0.003
Exp-T4	0.085	0.003
Exp-T5[a]	0.10	0.003
Exp-T6	0.125	0.003
Exp-T7	0.15	0.003
Exp-T8	0.175	0.003
Exp-T9	0.20	0.003

[a] Also used for the study to understand the difference between aerogel and xerogel

important material variables that play very important role in determining gelation, physical, mechanical, and thermal properties. Table 2 provides the detailed recipe used for the experiment. Some of these recipes were chosen to compare the difference between pDCPD based aerogel and xerogel. Also, in order to find the optimum values of target density and Grubbs catalyst content, we conducted a 2 variable 3 level 9 simple full factorial DOE experiment. Table 3 summarizes the material variables and levels used for the DOE experiment. The objective of DOE method used in this study is to quantitatively analyze the effects of these material variables on the important properties of the resultant pDCPD based aerogels. Statisca™ (StatSoft®) DOE software was used for experimental design and data analysis.

3 Results and discussion

It was observed that during gelation there was a phase transition from the transparent purple DCPD solution to an opaque pDCPD gel. The opaqueness is a result of light scattering by the polymerized DCPD. The accepted

Table 3 Material variables and levels used for a simple 3 level 2 factor 9 experiment full factorial DOE method

Experiment number	Factor 1 ρ_{Target} (g/cm^3)	Factor 2 Catalyst/DCPD (wt/wt)
DOE-1	0.04	0.003
DOE-2	0.04	0.0065
DOE-3	0.04	0.01
DOE-4	0.07	0.003
DOE-5	0.07	0.0065
DOE-6	0.07	0.01
DOE-7	0.1	0.003
DOE-8	0.1	0.0065
DOE-9	0.1	0.01

mechanism for the formation of the crosslinked pDCPD polymer is that the polymerization of the strained norbornene ring occurred first, followed by the subsequent metathesis of the cyclopentene unit, as Davidson and Wagener described [32]. They also reported that when the different types of catalysts such as the classical tungsten complex and Schrock's molybdenum alkylidene and the different concentration of toluene solvent were used, the linear soluble and/or crosslinked insoluble DCPD polymers could be formed depending on catalyst type and the solid content [32]. Based on their study, we may assume that when Grubbs catalysts are used, the linear and crosslinked DCPD polymers may coexist as shown in Fig. 3. The uniform pDCPD wet gels were formed and their aerogel monoliths were produced after supercritical drying. Uniform gelation is the most important prerequisite property for producing any types of organic and inorganic polymer based aerogels. Most of the pDCPD aerogel monoliths were produced with regular shape and appearance. However, it should be also noted that pDCPD aerogel samples prepared with lower target densities (i.e., 0.02 g/cm^3) became significantly shrunken after processing and did not show regular shape and appearance, generating dust due to their structural weaknesses. On the other hand, pDCPD aerogel monoliths prepared with relatively high target

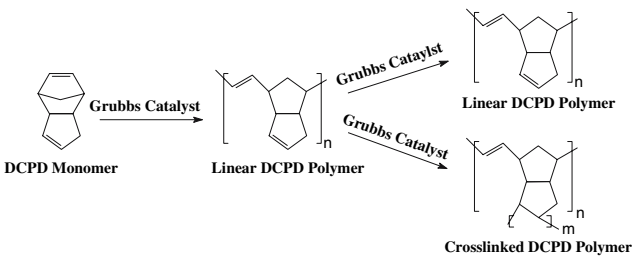

Fig. 3 The schematic illustration of the assembly for the thermal measurement system used in this study

density (i.e., 0.2 g/cm^3) were also shrunken non-uniformly in the radial direction, exhibiting some warpage of the sample surface. This is probably due to the different crosslinking reaction rates locally, inducing non-uniform structural stresses during aging.

Figure 4 provides the effects of the catalyst content at a constant target density of 0.06 g/cm^3 and the target density at a constant catalyst content of 0.003 as a ratio of Catalyst/DCPD (wt/wt) on the gelation kinetics for the resultant pDCPD wet gel formation, along with the best fit curve. However, it was difficult to accurately measure the gel times of pDCPD wet gels prepared with low catalyst content and target density, because their gelation occurred too slowly and gel states are too weak to determine gel point [33]. The gelation kinetics is well described by a 3-parameter exponential decay function, as indicated by high R^2 values of the fitting curves:

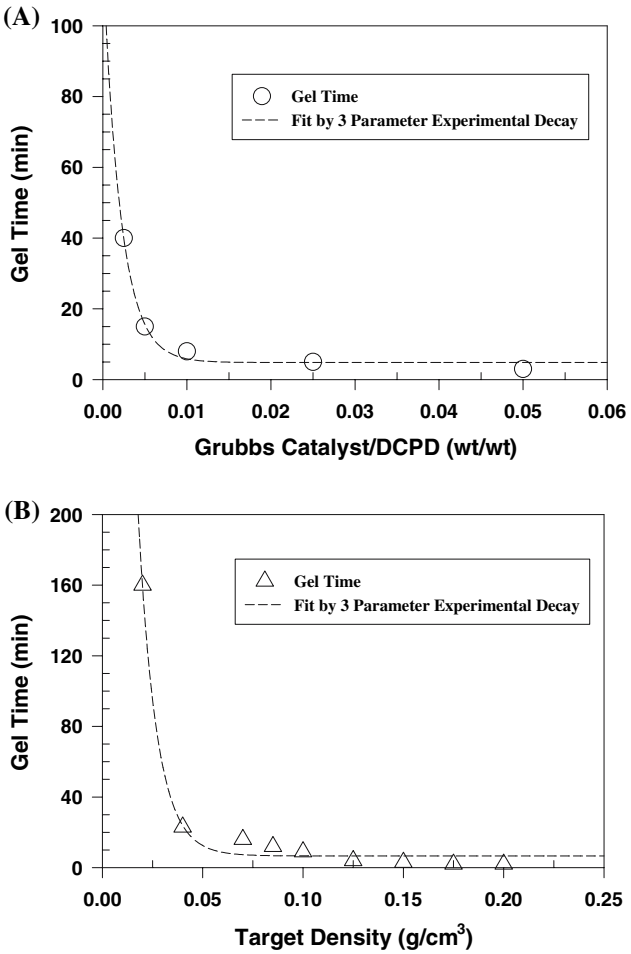

Fig. 4 The effects of the catalyst content at a constant target density of 0.06 g/cm^3 (**A**) and the effects of target density at a constant catalyst content of Catalyst/DCPD (wt/wt) = 0.003 (**B**) on the gel time of the pDCPD wet gel formation, along with the best fit curve

$$\text{Gel Time (min)} = 4.8 + 1.17e^{-4.7\text{Cat.}} \quad (\text{Gel Time vs. Catalyst Content, } R^2 = 0.9908) \tag{1}$$

$$\text{Gel Time (min)} = 6.6 + 1.4e^{-1.1\text{TD}} \quad (\text{Gel Time vs. Target Density, } R^2 = 0.9917) \tag{2}$$

During gelation there was a phase transition from the transparent purple DCPD solution to an opaque gel due to the light scattering by the polymerized pDCPD wet gel. Table 4 demonstrates the final density, shrinkage factor, porosity, and thermal conductivity values of the pDCPD aerogels prepared with a constant target density of 0.06 g/cm^3 as a function of catalyst content used. As shown by the data in Table 4, our first pDCPD aerogel monoliths exhibited low shrinkage factors of <1.6, relatively high porosities of over 90%, and good thermal conductivity values of less than 25 mW/m K. However, the variations of thermal conductivity values at the different locations over the pDCPD aerogel samples are higher than those typically measured for silica aerogel materials, generally less than 1 mW/m K. These thermal conductivity differences could be manifested due to non-uniform pore structures formed over the pDCPD aerogel volume. Note that the porosities were calculated from the bulk density (see Experimental section) using the measured material density. Additional discussion on detailed pore structures and morphologies of pDCPD aerogel monoliths will be provided later. Overall, as more catalyst is incorporated, higher shrinkage factors (i.e., final density), slightly lower porosities, and slightly better thermal conductivity values are likely observed from the resultant pDCPD aerogel probably due to their densely crosslinked structure and smaller pores.

The effect of the target density on the important properties of the resultant pDCPD aerogel samples prepared with a constant catalyst content of Catalyst/DCPD (wt/wt) = 0.003 was also investigated, as summarized in Table 5. It is observed from Table 5 that as target density (i.e., solid content) is increased, the gel times decrease and the resultant gels exhibit less porosity and also lower

Table 4 Results of the final density, shrinkage factor, porosity, and thermal conductivity values of the pDCPD aerogel prepared with a constant target density of 0.06 g/cm^3 as a function of catalyst content

Experiment number	Final density (g/cm^3)	Shrinkage Factor	Porosity (%)	Thermal conductivity (mW/m K)
Exp-C1	0.0693	1.16	93.5	24.9 ± 2.3
Exp-C2	0.0894	1.49	91.6	24.8 ± 1.5
Exp-C3	0.0829	1.38	92.2	21.5 ± 1.7
Exp-C4	0.0855	1.43	92.0	21.2 ± 1.8
Exp-C5	0.0939	1.57	91.0	22.9 ± 1.2

Table 5 Results of the final density, shrinkage factor, porosity, and thermal conductivity values of the pDCPD based aerogel prepared with a constant Grubbs catalyst content of catalyst/DCPD (wt/wt) = 0.003 as a function of target density

Experiment number	Gel time (min)	Shrinkage factor	Porosity (%)	Thermal conductivity (mW/m K)
Exp-T1	160	N/A[2]	N/A[b]	N/A[b]
Exp-T2	23	1.62	93.91	28.3 ± 2.2
Exp-T3	16	1.22	91.97	23.7 ± 1.2
Exp-T4	12	1.35	89.22	20.2 ± 1.0
Exp-T5	9	1.50	85.90	19.7 ± 1.7
Exp-T6	4	1.71	79.91	17.9 ± 1.5
Exp-T7	3	1.89	73.36	16.6 ± 1.4
Exp-T8	2[a]	2.26	62.83	N/A[c]
Exp-T9	2[a]	2.45	53.95	N/A[c]

[a] Difficult to accurately measure due to the fast gelation

[b] The broken aerogel was produced after supercritical drying due to its weakness

[c] The warpage of sample occurred due to the irregular deformation

thermal conductivity values. Lower shrinkage factors were observed from samples prepared with target density of 0.07 g/cm^3 indicating the existence of an optimum point. If higher target density is used, faster ROMP reaction occurs due to more DCPD monomers in the solution, which generally results fast gelation, lower porosities, smaller pore sizes, and lower thermal conductivity values of the resultant pDCPD aerogels. Lower thermal conductivity values at higher density may obtain due to lower gas conduction and radiation contribution relative to the increasing solid thermal conductivity contribution. Figure 5 provides the behaviors of thermal conductivity values

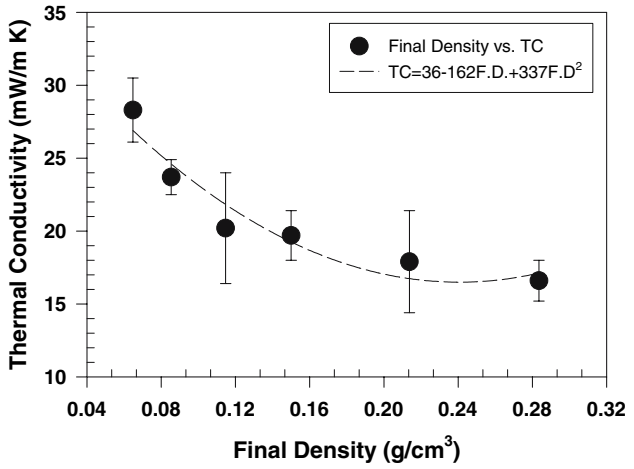

Fig. 5 Thermal conductivity values of pDCPD aerogels prepared with a constant catalysts content of Catalyst/DCPD (wt/wt) = 0.003 as a function of the final density

of pDCPD aerogels prepared with a constant catalyst content of Catalyst/DCPD (wt/wt) = 0.003 as a function of the final density along with best fitting curve. It is clearly observed from Fig. 5 that pDCPD aerogel shows decreasing thermal conductivity value with increasing target density, possibly indicating the minimum thermal conductivity value at the final density around 0.22 g/cm^3. Earlier, Lu et al. [20] investigated the thermal conductivity of the organic polymer based resorcinol-formaldehyde aerogel and reported the lowest thermal conductivity values at density of around 0.16 g/cm^3 in air. Also, Hummer et al. [34] observed the minimum total thermal conductivity values of the opacified silica aerogel powders at density of around 0.12 g/cm^3. The specific final densities to exhibit the minimum thermal conductivity of the different types of aerogels may be associated with material characteristics and pore structure and morphology. A more detailed description of the relationship between the resultant thermal conductivity value of aerogel and heat transfer mechanisms such as solid conduction, gaseous conduction, and radiation conduction as a function of the final density can be found in a paper by Hummer et al. [34]. Although our pDCPD aerogel demonstrated similar thermal conductivity behavior as a function of the final density to other aerogel materials characterized in the literature, the minimum thermal conductivity values found for pDCPD aerogel of about 16.5 mW/m K is slightly higher than those of resorcinol-formaldehyde aerogel monolith (12 mW/m K) and opacified silica aerogel (13 mW/m K).

PDCPD based aerogels and xerogels made during the course of this study were measured for their shrinkage factor and thermal conductivity values. Table 6 provides a comparison of typical properties of pDCPD aerogel and xerogel prepared after supercritical and ambient drying respectively (e.g. Exp-T5), while Fig. 6 shows pDCPD aerogel with bright color and xerogel monoliths with dark colors clearly exhibiting different amounts of shrinkage due to different density. Xerogels were typically prepared by drying for about 2 months at ambient conditions at which point no more volume change was observed. It is clear from Table 6 and Fig. 6 that xerogels are character-

Table 6 The comparison of typical properties of pDCPD aerogel and xerogels

Exp	Shrinkage factor	Porosity (%)	Thermal conductivity (mW/m K)
Aerogel	1.35	87.3	20.3 ± 1.5
Xerogel-1	5.56	38.3	52.5 ± 3.8
Xerogel-2	4.89	44.6	44.7 ± 4.6[a]

[a] Less accurate result is expected due to less uniform sample shape, although the flat surface was used for measurement

Fig. 6 Demonstration of pDCPD aerogel and xerogels showing the different appearances resulted from the different shrinkage occurred due to the different drying methods applied

ized with higher final densities (i.e., higher shrinkage factor), lower porosity, and higher thermal conductivity due to their higher solid conduction [30]. As discussed earlier, the capillary pressure during drying plays the most important role in determining these pDCPD aerogel and xerogel materials [8–12]. It should be noted that xerogels do not represent bulk material, but typically contain far fewer pores, lower surface area, and smaller pore volume than corresponding aerogels. As a result of lower porosity, the pDCPD xerogels are generally stronger, stiffer, and more brittle than their aerogel counterparts. The shrinkage of xerogels depends strongly on the target density (i.e., solid content) used for preparations. It should be also noted that since pDCPD bulk polymer exhibits excellent mechanical strength, toughness, and intrinsic hydrophobicity, obtaining pDCPD xerogels with good appearance is relatively easy compared to silica xerogels which are easily broken or cracked during drying [35].

To find the optimum target density and Grubbs catalyst contents, a DOE experiment was conducted as shown in Table 3. The effects of target density and Grubbs catalyst content on gel time, and shrinkage factor and thermal conductivity values measured at room temperature were numerically analyzed and summarized in Table 7. It is observed from Table 7 that the experimental and predicted gel time, porosity, and thermal conductivity are quite consistent. A slight differences between experimental and predicted values are generally observed from samples prepared with relatively lower target density and catalyst content. The irregular shrinkage (deformed shape) and the resulting changes to pore structure appear to be affected by processing variables such as mixing intensity and time, aging period and temperature, and supercritical drying conditions. Slight variations in these factors may be responsible for the discrepancies observed between experimental and DOE predictions for these samples. Figure 7 provides the schematic illustration of effects of target density and catalyst content on the gel time, porosity, and thermal conductivity of the resultant pDCPD aerogel. Note that for comparison purposes, the Y axis for each property has the same scale and thus, effects of these variables can be directly compared from the length and slope of curves. It is clearly observed from Fig. 7 that target density and catalyst content play an important role in determining the gel time and the thermal conductivity values of the resultant pDCPD aerogels, while the overall porosity is not significantly affected by catalyst content. As target density and catalyst content are increased, faster gel time and lower thermal conductivity are observed from the resultant pDCPD aerogels. It is also likely to show that the target density plays a more important role in determining porosity and thermal conductivity than catalyst content, while the gel time is slightly more affected by catalyst content. The effects of these material variables on important properties are very consistent with previous results conducted separately, as shown in Table 4, Table 5, and

Table 7 Results of the important properties such as gel time, shrinkage, and thermal conductivity values of pDCPD samples conducted with DOE method comparing with predictions by DOE program

Experiment number	Gel time (min)	Prediction by DOE ($R^2 = 0.98$)	Porosity (%)	Prediction by DOE ($R^2 = 0.96$)	Thermal conductivity (mW/m K)	Prediction by DOE ($R^2 = 0.95$)
DOE-1	19.0	18.0	93.5	93.6	27.1 ± 3.2	25.9
DOE-2	11.0	11.3	93.8	93.8	22.9 ± 1.2	23.9
DOE-3	8.0	8.7	93.8	93.8	23.4 ± 3.0	23.7
DOE-4	16.0	15.7	91.3	90.4	20.5 ± 2.2	22.1
DOE-5	9.0	9.0	89.5	90.6	20.9 ± 3.9	20.2
DOE-6	6.0	6.3	90.7	90.6	20.8 ± 2.3	19.9
DOE-7	9.0	10.3	85.0	85.8	17.5 ± 2.7	17.1
DOE-8	4.0	3.7	87.0	86.0	15.4 ± 2.1	15.2
DOE-9	2.0	1.0	85.8	86.0	14.3 ± 2.0	14.9

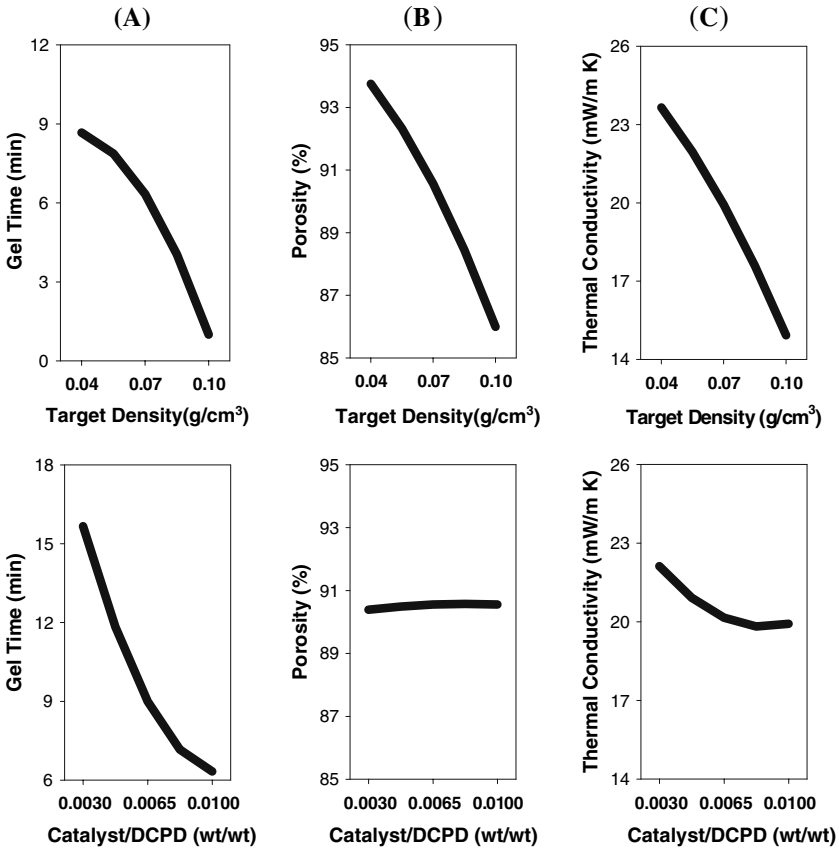

Fig. 7 Schematic illustration of the effects of target density and catalyst content on the gel time (**A**), porosity (**B**), and thermal conductivity (**C**) as provided by the DOE analysis program

Fig. 5. The relationships between material variables and gel time, the porosity, and thermal conductivity value obtained are shown in Eqs. (3–5), respectively:

$$\text{Gel Time (min)} = 25 + 106X_1 - 3456X_2 - 1668X_1^2 + 163249X_2^2 \quad (3)$$

$$\text{Porosity}(\%) = 95 - 24X_1 + 109X_2 - 755X_1^2 - 6566X_2^2 \quad (4)$$

$$\text{Thermal Conductivity (mW/m K)} = 32 - 47X_1 - 1244X_2 - 706X_1^2 + 71620X_2^2 \quad (5)$$

where X_1 and X_2 are target density and catalyst content as a weight ratio of Grubbs Catalyst/DCPD, respectively. The gel time, porosity, and thermal conductivity predicted with Eqs. (3–5) are included in Table 7 with experimental results, as discussed earlier. More detailed DOE method can be found in [36].

Figure 8 demonstrates differential scanning calorimetry (DSC) behavior of several pDCPD aerogels prepared with different target densities and Grubbs catalyst contents along with two 2nd runs of one pDCPD aerogel sample. Figure 8 clearly shows that pDCPD aerogel prepared with target density of 0.06 g/cm^3 and a catalyst content of cat-

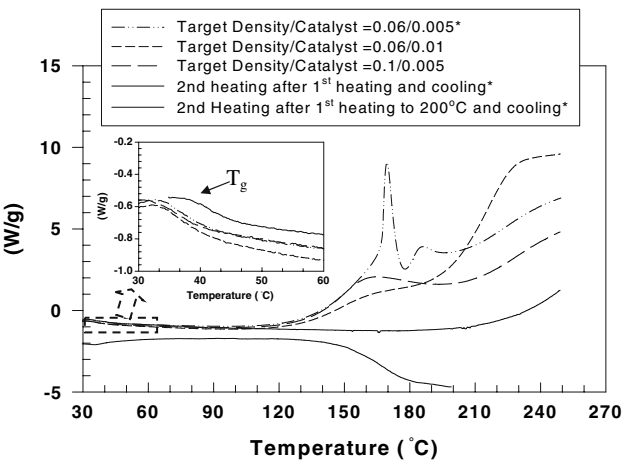

Fig. 8 Demonstration of DSC behaviors of pDCPD aerogel prepared with different target densities and Grubbs catalyst contents along with thermal behavior after 2nd run

Table 8 Densities, nanopore volumes, average sizes, surface areas, and thermal conductivity values of pDCPD aerogel comparing with different types of aerogels

Samples	Density (g/cc)	Pore volume (cm^3/g)	Average pore diameter (nm)	Surface area (m^2/g)	Thermal conductivity (mW/m K)
PDCPD DOE2[a]	0.0656	0.89	15.1	235	22.9
PDCPD DOE5[a]	0.1117	1.07	17.4	245	20.9
PDCPD DOE8[a]	0.1379	1.00	18.0	221	15.4
Polyurethane[a]	0.1277	0.16	13.0	47	27.0
Polyisocyanurate[a]	0.1247	0.59	8.5	282	19.0
Silica Aerogel[b]	0.0902	2.86	13.7	686	12.0

[a] Degassing at temperature of 70 °C for 12 h under the vacuum

[b] Degassing at temperature of 105 °C for 12 h under the vacuum

alyst/DCPD (wt/wt) = 0.005 exhibits a relatively broad curve at around 37 °C (probably representing a glass-transition temperature (T_g)) and two sharp exothermic peaks between 120 and 200 °C. The exothermic peaks are typically observed for pDCPD aerogels with low or medium target density up to 0.08 g/cm^3 and a catalyst content of catalyst/DCPD = 0.005. If higher target density and catalyst content are used, higher ROMP reaction occurred during preparation and thus these exothermic peaks become less significant due to less components unreacted, as observed from Fig. 8. The low T_gs of around 35–45°C observed from our pDCPD aerogels are consistent with those of the linear DCPD polymer reported in the literature. For example, Abadie et al. [37] obtained T_g of 53 °C from the linear DCPD polymer and Kessler and White [27] observed T_g of between 29 and 49 °C from the samples that incorporated different catalyst content. Also, since it is known that T_g of the fully cured pDCPD bulk samples is around 139 °C [27], from the DSC trace in Fig. 8 it could be considered that the T_g of the crosslinked pDCPD aerogel is obscured by the sharp exothermic reaction peaks between 120 and 200 °C. Because the pDCPD aerogel samples prepared are not soluble in toluene, we may conclude that they consist of both the linear and crosslinked polymers. Running a DSC scan after one heating cycle no longer shows any the exothermic peaks and likely exhibits T_g of the fully cured pDCPD aerogel between 150 and 180 °C. In order to increase the overall polymerization reaction during sample preparation, Wooden and Grubbs [38] suggested that the DCPD starting material may optionally include one or more crosslinking agents for initiating additional crosslinking of the pDCPD. More detailed investigations for the relationship between the resultant pDCPD aerogel structure and thermal behavior will be the focus of future studies.

The thermal conductivity values of aerogels are greatly affected by the distribution and morphology of their nanopore structures, nanopore volume, surface area, and size, formed during material preparation. Table 8 provides densities, nanopore volumes, average sizes, surface areas, and thermal conductivity values of pDCPD aerogels comparing with those of different types of organic and silica

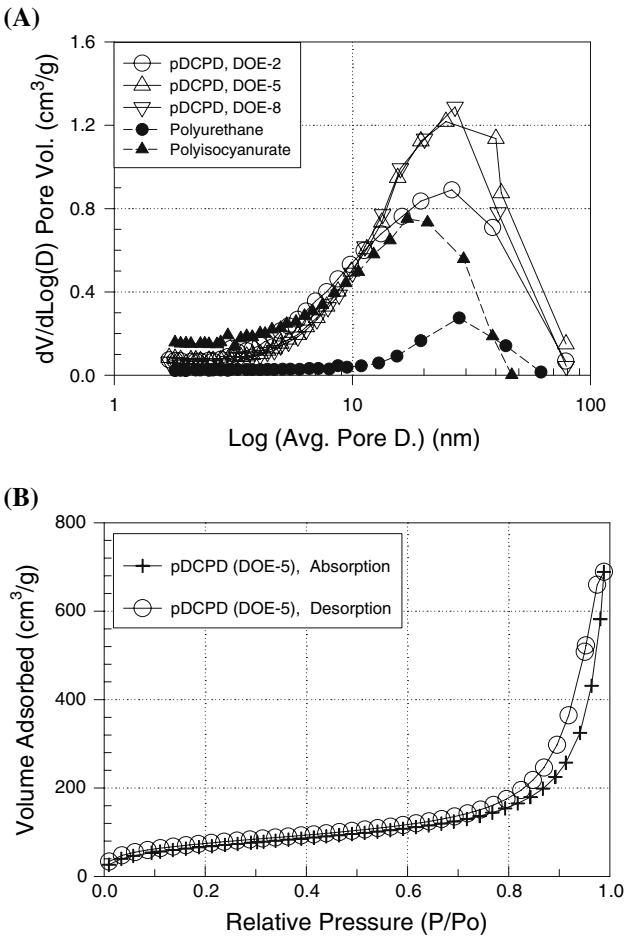

Fig. 9 Demonstration of the relationship between pore size (Log (average pore diameter)) and pore volume (Barrett, Joyner, and Halenda (BJH) Desorption Pore Volume, dV/dlog(D)) of pDCPD aerogel at a constant catalyst content of catalyst/DCPD (wt/wt) = 0.0065 as a function of target density (**A**) and the adsorption and desorption isotherm for a pDCPD aerogel of DOE-5 (**B**)

aerogels. A relatively low degassing temperature of 70 °C was used for BET and pore size analysis of organic aerogels including pDCPD aerogels, while a degassing temperature of 105 °C was used for analysis of silica aerogels (see Experimental section). It is observed from Table 8 that silica aerogel shows the highest nanopore volume and surface area, followed by pDCPD aerogels, while polyurethane aerogels exhibited the least nanopore volume and surface area. The lowest and highest thermal conductivity values exhibited by silica and polyurethane aerogels respectively, are likely associated with differences in their nanopore volumes and surface areas. The pore volume and surface area observed from our polyurethane aerogel are very consistent with those investigated by Rigacci et al. [21]. On the other hand, pDCPD and polyisocyanurate aerogels with similar density demonstrate comparable thermal conductivity values. As observed from Table 8, pDCPD aerogels contained almost two times the pore volume of polyisocyanurate aerogel, while smaller pores are included in polyisocyanurate aerogel as indicated by smaller average diameter and larger surface area of nanopores. As a result, it may be considered that the size and surface area of nanopores included in aerogel materials also have a close relationship with their thermal conductivity values. Figure 9 demonstrates the effect of target density on the pore size distribution of pDCPD aerogel prepared with a constant catalyst content of catalyst/DCPD (wt/wt) = 0.0065 comparing with those of polyurethane and polyisocyanurate aerogels and the adsorption and desorption isotherm behaviors of a pDCPD aerogel of DOE-5. It is clearly observed from Fig. 9 that pDCPD aerogels have wider pore size distribution than those of polyurethane and polyisocyanurate aerogels, mainly in the regions indicating larger pores. Polyisocyanurate aerogel contains a greater distribution of smaller pores (<10 nm) than other aerogels studied. As a higher target density is used, fewer small pores are formed in samples of polyisocyanurate aerogel, while larger pores increased in the resultant pDCPD aerogel. As a result, although the pore volume increased with increasing target density, the overall pore size distribution was not significantly changed by changes in target density. Our results are not consistent with the prevailing wisdom that smaller pore size is generally observed from aerogels with higher density [35]. The absorption and desorption behavior measured as a function of relative pressure, demonstrates a typical shape of the porous solid with pore shape of rod and/or spherical holes [39].

Figure 10 shows SEM results and illustrates the pore morphologies of pDCPD aerogels with two different densities (DOE-2 and DOE-8) measured at relatively low magnifications of ×10K comparing with those of polyurethane and silica aerogels. Pore morphologies measured at relatively higher magnifications of ×60K are given in Fig. 11. We were hoping to correlate the thermal conductivity values of pDCPD aerogels with their general nanopore structure by comparing with silica and polyurethane aerogel morphologies respectively. It is observed from Figs. 10 and 11 that silica aerogel shows the finest nanopore morphology, followed by high density pDCPD aerogel of DOE 8, while low density pDCPD aerogel of DOE 2 and polyurethane aerogels exhibit less uniform tangle or web-like morphologies containing macroscale pores. These large pores observed from these low density pDCPD and

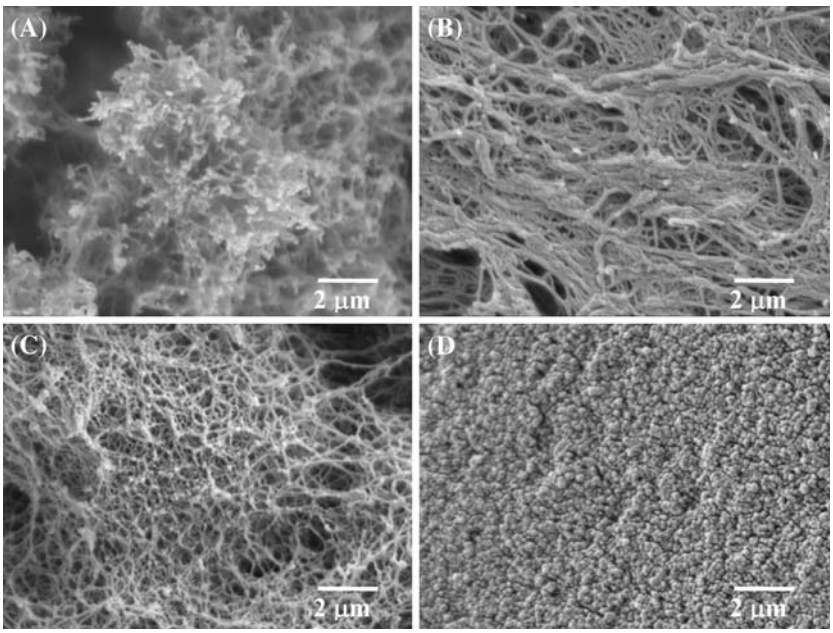

Fig. 10 Pore morphologies of pDCPD aerogels with two different densities of DOE-2 (**A**) and DOE-8 (**B**) measured at relatively lower magnification of ×10K comparing with those of polyurethane (**C**) and silica (**D**) aerogels

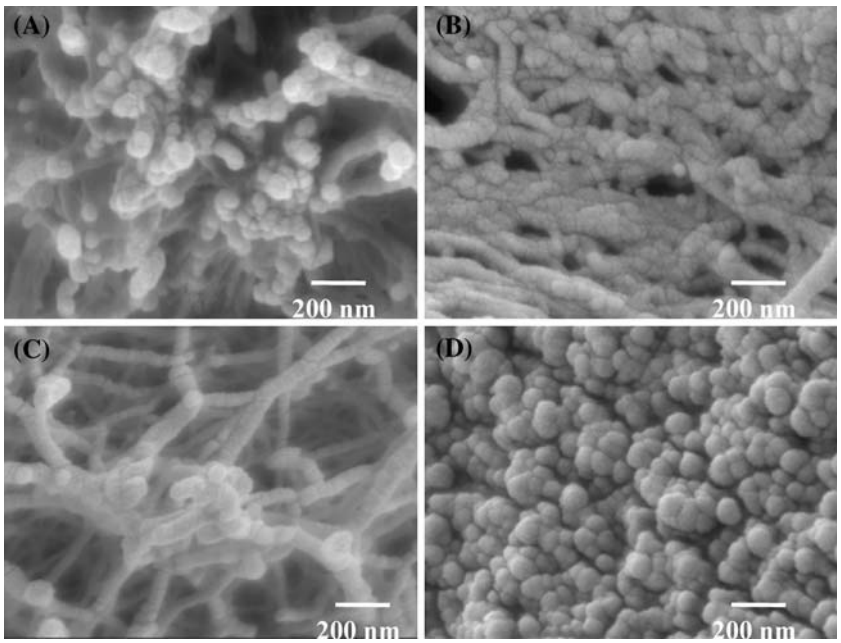

Fig. 11 Pore morphologies of pDCPD aerogels prepared with two different densities of DOE-2 (**A**) and DOE-8 (**B**) measured at relatively higher magnification of ×60K comparing with those of polyurethane (**C**) and silica (**D**) aerogels

polyurethane organic aerogels may occur due to less uniformly developed gel structure or entrapping air bubbles during processing. Many large pore structures (possibly defects) observed by SEM in pDCPD and polyurethane aerogels may increase their gaseous and radiation thermal conductivity contributions [40]. In order to significantly improve the thermal conductivity of pDCPD aerogels, especially low density pDCPD aerogels, further optimization of processing methods will be required focusing on the relationship between large pores and thermal conductivity.

4 Conclusion

In this study we demonstrated that lightweight nanoporous pDCPD based aerogels can be produced by using a simple sol-gel processing and supercritical drying method. The uniform pDCPD gels were formed by ROMP with a Grubbs type Ru-catalyst at room temperature and atmospheric pressure. Supercritical CO_2 drying was used to produce pDCPD aerogels from the wet gel materials. The pDCPD based aerogels exhibited a wide range of final densities and had high porosity (including mesoporosity), lower thermal conductivities, and inherent hydrophobic due to their nanopored hydrocarbon structures. Both target density and catalyst content played very important roles in determining important properties of the resultant pDCPD aerogels. At higher target density and catalyst content, it was observed that gel times were faster and thermal conductivity values were lower. Compared with pDCPD xerogels, pDCPD aerogels are characterized with lower final densities (i.e., smaller shrinkage factor), higher porosity, and lower thermal conductivity values. DSC and solvent extraction studies indicated the coexistence of linear and the crosslinked polymers in the aerogel materials. The newly prepared pDCPD aerogels are very promising candidates for many thermal and acoustic insulation applications including cryogenic insulation.

Acknowledgment This work was conducted by the financial support of the United States Defense Advanced Research Projects Agency (DARPA), SBIR Contract No. W31P4Q-05-C-0231. The authors are grateful to Mr. Max Mesham, Ms. Geeta Bhakhari, and Mr. Nathan Bhobho for their helps in preparing samples and also, to Ms. Sara Rosenberg, Dr. Shannon White, and Dr. Jeffrey Boehme for their valuable helps. The authors would like to thank Dr. Karen Wood in DARPA for her continuous supports for this work. The authors are also grateful to Dow Corning Analytical Lab for SEM measurement.

References

1. Kistler SS (1931) Nature 127:741
2. Kistler SS (1932) J Physical Chem 36:52
3. LeMay JD, Hopper RW, Hrubesh LW, Pekala RW, MRS Bulletin, December 1990, p 19
4. Schaefer D, MRS Bulletin, April 1994, p 49
5. Hrubesh LW, Poco JF (1995) J Non-Cryst Solids 188:46
6. Schmidt M, Schwertfeger F (1998) J Non-Cryst Solids 225:364
7. Fricke J, Emmerling A (1998) J Sol-Gel Sci Tech 13:299
8. Hüsing N, Schubert U (1998) Angrew Chem Int Ed 37:22
9. Pierre AC, Pajonk GM (2002) Chem Rev 102:4243
10. Akimov YK (2003) Instrum Exp Tech 46:287
11. Pajonk GM (2003) Colloid Polym Sci 281:637
12. Bisson A, Rigacci A, Lecomte D, Rodier E, Achard P (2003) Drying Technol 21:593
13. Pekala RW, Schaefer DW (1993) Macromolecules 26:5487
14. Pekala RW (1989) J Mater Sci 24:3221
15. Pekala RW, Kong FM (1989) Polym Prepr 30:221

16. Ward RL, Pekala RW (1990) Polym Prepr 31:167
17. Pekala RW, Alviso CT, LeMay JD (1990) J Non-Cryst Solids 125:67
18. Pekala RW, Alviso CT, Kong FM, Hulsey SS (1992) J Non-Cryst Solids 145:90
19. Lu X, Arduini-Schuster MC, Kuhn J, Nilsson O, Fricke J, Pekala RW (1992) Science 255:971
20. Lu X, Caps R, Fricke J, Alviso CT, Pekala RW (1995) J Non-Cryst Solids 188:226
21. Rigacci A, Marechal JC, Repoux M, Moreno M, Achard P (2004) J Non-Cryst Solids 350:372
22. Biesmans G, Randall D, Francais E, Perrut M (1998) J Non-Cryst Solids 225:36
23. Biesmans G, Mertens A, Duffours L, Woignier T, Phalippou J (1998) J Non-Cryst Solids 225:64
24. Fischer F, Rigarcci A, Pirad R, Berthon-Fabry S, Achard P (2006) Polymer 47:7636
25. Tan C, Fung BM, Newman JK, Vu C (2001) Adv Mater 13:644
26. Hine PJ, Leejarkpai T, Khosravi E, Duckett RA, Feast WJ (2001) Polymer 42:9413
27. Kessler MR, White SR (2002) J Polym Sci Part A: Polym Chem 40:2373
28. Furstner A (2000) Angew Chem Int Ed 39:3012
29. Grubbs RH (2004) Tetrahedron 60:7117
30. Lee JK, Mesham M, Chittick H, Gould GL, DARPA SBIR Phase I Contract No. W31P4Q-04-C-R087, Final Report, September (2004)
31. Martina AD, Hilborn JG, Mu1hlebach A (2002) Macromolecules 33:2916
32. Davidson TA, Wagener KB (1998) J Mol Catal A 133:67
33. Lee JK, Gould GL (2005) J Sol-Gel Sci Tech 34:281
34. Hummer E, Rettelbach T, Lu X, Fricke J (1993) Thermochimica Acta 218:269
35. Brinker CJ, Scherer GW (1990) Sol-Gel Science Ch 9. Academic Press, San Diego
36. Program Manuals of Statisca, Vol. IV Industrial statistics, Experimental design, StatSoft (1995), p 4254
37. Abadie MJ, Dimonie M, Couve C, Dragutan V (2000) Eur Polym J 36:1213
38. Grubbs RH, Woodson CS, USP 6,020,443 and USP 5728785
39. Paul A, Clyde O (1997) Analytical methods in fine particle technology Ch 3. Micrometrics Instrument, Norcross GA
40. Lee OJ, Lee KH, Kim SY, Yoo KP (2002) J Non-Cryst Solids 298:287